CHEMISTRY
A EUROPEAN JOURNAL

FULL PAPER

DOI: 10.1002/chem.201301280

# Cooperative Catalysis of Metal and O−H···O/sp$^3$-C−H···O Two-Point Hydrogen Bonds in Alcoholic Solvents: Cu-Catalyzed Enantioselective Direct Alkynylation of Aldehydes with Terminal Alkynes

**Takaoki Ishii,[a] Ryo Watanabe,[b] Toshimitsu Moriya,[a] Hirohisa Ohmiya,[a] Seiji Mori,*[b] and Masaya Sawamura*[a]**

*Dedicated to Professor Teruaki Mukaiyama in celebration of the 40th anniversary of the development of the Mukaiyama aldol reaction*

**Abstract:** Catalyst–substrate hydrogen bonds in artificial catalysts usually occur in aprotic solvents, but not in protic solvents, in contrast to enzymatic catalysis. We report a case in which ligand–substrate hydrogen-bonding interactions cooperate with a transition-metal center in alcoholic solvents for enantioselective catalysis. Copper(I) complexes with prolinol-based hydroxy amino phosphane chiral ligands catalytically promoted the direct alkynylation of aldehydes with terminal alkynes in alcoholic solvents to afford nonracemic secondary propargylic alcohols with high enantioselectivities. Quantum-mechanical calculations of enantiodiscriminating transition states show the occurrence of a nonclassical sp$^3$-C−H···O hydrogen bond as a secondary interaction between the ligand and substrate, which results in highly directional catalyst–substrate two-point hydrogen bonding.

**Keywords:** asymmetric catalysis · cooperative catalysis · copper · density functional calculations · hydrogen bonds

## Introduction

Directional hydrogen bonds are the central element of enzymatic catalysis by stabilizing a transition state in a chemo- and stereocontrolled manner.[1] Chemists can utilize this information to design hydrogen bonds in an effort to develop artificial catalysts. In fact, various enantioselective artificial catalysts reminiscent of enzymes have been developed to date.[2–5] However, catalyst–substrate hydrogen bonds in artificial catalysts usually occur in aprotic solvents[6–8] or in organic/aqueous biphasic systems[9,10] in contrast to enzymatic catalysis in aqueous media.[11]

Herein, we report the enantioselective direct alkynylation of aldehydes with terminal alkynes[12–16] catalyzed by copper(I) complexes with prolinol-based hydroxyamino phosphane chiral ligands and present experimental and computational evidence for directional hydrogen-bonding interactions between chiral catalysts and substrates in alcoholic solvents. This cooperative catalysis provides an efficient method to access a wide range of enantioenriched secondary propargylic alcohols that are versatile synthetic intermediates for more complex nonracemic compounds.[17,18] A hydroxy group of the ligand plays a critical role in promoting the reaction, and protic solvents promote a favorable reaction rate and enantioselectivity. Guided by quantum-mechanical calculations, we propose the existence of a nonclassical sp$^3$-C−H···O hydrogen bond as a secondary interaction between the ligand and substrate, which results in highly directional catalyst–substrate two-point hydrogen-bonding.

The catalytic enantioselective addition of terminal alkynes to aldehydes is an important C−C bond-formation reaction to prepare enantioenriched secondary propargylic alcohols that are versatile synthetic intermediates. To date, the Zn-(OTf)$_2$/*N*-methylephedrine/Et$_3$N,[13] In$^{III}$/1,1′-bi-2-naphthol (BINOL)/Cy$_2$NMe (Cy = cyclohexyl),[14] and Ru$^{II}$/bis(oxazolinyl)arene[16] systems have been developed by Carreira, Shibasaki, and Nishiyama. These systems, however, have problems, such as limited substrate scope or use of precious metals and organic bases in large quantities. In contrast, our protocol uses a base metal copper and a natural amino acid-derived chiral ligand and is applicable for both aliphatic and aromatic aldehydes in combination with various types of alkynes, thus eliminating the problems of the reported systems.[19]

[a] T. Ishii, T. Moriya, Prof. Dr. H. Ohmiya, Prof. Dr. M. Sawamura
Department of Chemistry
Faculty of Science, Hokkaido University
Sapporo 060-0810 (Japan)
Fax: (+81) 11-706-3749
E-mail: sawamura@sci.hokudai.ac.jp

[b] R. Watanabe, Prof. Dr. S. Mori
Faculty of Science, Ibaraki University
Mito 310-8512 (Japan)
E-mail: smori@mx.ibaraki.ac.jp

Supporting information for this article is available on the WWW under http://dx.doi.org/10.1002/chem.201301280.

## Results and Discussion

**Design of hydrogen-bonding-based catalysts**: An earlier investigation on the $Cu^{I}$-catalyzed enantioselective addition of terminal alkynes to aldehydes identified the TRAP[20] class of chiral bisphosphanes as effective ligands to render a catalytically active $Cu^{I}$ complex that promotes alkynylation under mild conditions[15] (Figure 1 a). Unfortunately, the substrate scope was limited to aromatic aldehydes and phenylacetylene derivatives, and the obtained enantioselectivities were only moderate.

The design of a second-generation catalyst system was based on a previous observation that the use of alcoholic solvents gave better reaction rates and enantioselectivities than aprotic solvents. This finding implies the cooperation of an alcoholic solvent molecule through a six-centered transition state (Figure 1 a) and prompted us to develop a Cu-based chiral catalyst that incorporates an alcoholic hydrogen-bonding site and a phosphane-based bidentate coordination site within a chiral organic scaffold to promote well-defined ligand–substrate hydrogen bonding in the enantiodiscriminating transition state (Figure 1 b). By having an additional oxygen-based coordination site, such a hydroxylated phosphane ligand may be able to function as a tridentate ligand for the Cu center. We expected that the resulting tridentate coordination would enable monomerization of a $Cu^{I}$/acetylide complex without introducing a large-bite-angle chelating moiety as in the TRAP ligands.

Another important design concept was to place a pyramidal $sp^3$-hybridized atom rather than a planer $sp^2$-hybridized atom at the pivotal position that connects the phosphane and alcoholic sites, so that the chiral tridentate ligand fits to a tetrahedral geometry of the Cu center. These considerations identified a class of prolinol-based hydroxyamino phosphane **L** to be ideal (Figure 1 b).

**Optimization**: For the initial set of experiments, the prototype hydroxy amino phosphane chiral ligand **L1** (10 mol%) was used in combination with CuO*t*Bu (10 mol%) for the reaction between CyCHO (**1a**; 0.2 mmol) and HC≡CSi*i*Pr$_3$ (**2a**; 2 equiv) to give propargylic alcohol **3a** in various media, including nonpolar and polar aprotic solvents and protic solvents with a constant reaction time of 48 hours (the results are summarized in Table 1). To our delight, the reaction proceeded at 40 °C in aprotic solvents such as hexane, toluene, THF, DMF, and MeCN in low or moderate yields and enantioselectivities (Table 1, entries 1–5). In accord with the hydrogen-bonding-based catalyst design, change of the hydroxy group of **L1** into a methoxy group (**L1-OMe**) completely inhibited the reaction (toluene, 65 °C), thus indicating a critical role for the alcoholic site (Table 1, entry 6).

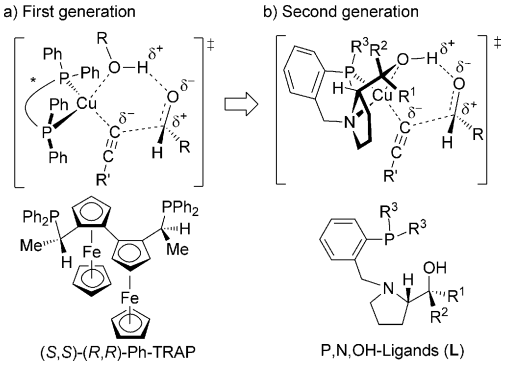


Figure 1. Cooperative transition state hypotheses: a) First and b) second generation.

Table 1. The effect of solvents and chiral ligands on the copper-catalyzed alkynylation of **1a** with **2a**.[a]

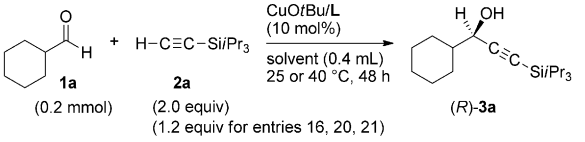


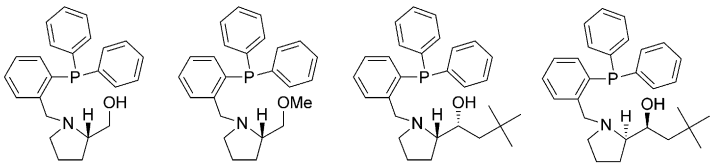


| Entry | Ligand | Solvent | *T* [°C] | Conversion of **1a** [%][a] | **3a** Yield [%][b] | e.r.[c] |
|---|---|---|---|---|---|---|
| 1 | **L1** | hexane | 40 | 42 | 37 | 67:33 |
| 2 | **L1** | toluene | 40 | 48 | 43 | 66:34 |
| 3 | **L1** | THF | 40 | 32 | 32 | 64:38 |
| 4 | **L1** | DMF | 40 | 15 | 15 | 68:32 |
| 5 | **L1** | MeCN | 40 | 19 | 18 | 72:28 |
| 6 | **L1-OMe** | toluene | 40 | 0 | 0 | N.A.[d] |
| 7 | **L1** | EtOH | 40 | 71 | 70 | 82:18 |
| 8 | **L1** | *i*PrOH | 40 | 92 | 92 | 83:17 |
| 9 | **L1** | *t*BuOH | 40 | 92 | 92 | 82:18 |
| 10 | **L1** | *i*PrOH | 25 (96 h) | 91 | 89 | 85:15 |
| 11 | **L1-OMe** | *t*BuOH | 40 | 0 | 0 | N.A.[d] |
| 12 | **L2** | *i*PrOH | 40 | 100 | 95 | 94:6 |
| 13 | **L2** | *i*PrOH | 25 | 100 | 99 | 95:5 |
| 14 | **L2** | *t*BuOH | 25 | 100 | 98 | 96:4 |
| 15 | **L2** | *t*BuOH + $H_2O$[e] | 25 | 100 | 98 | 97:3 |
| 16[f] | **L2** | *t*BuOH + $H_2O$[e] | 25 | 100 | 98 | 97:3 |
| 17 | ***ent*-L2** | *t*BuOH + $H_2O$[e] | 25 | 100 | 97 | 97:3 |
| 18 | **L2** | toluene | 40 | 54 | 48 | 78:22 |
| 19 | **L2** | THF | 40 | 29 | 24 | 67:23 |
| 20[f] | **L2** | *t*BuOH/toluene (3:1) | 25 | 100 | 98 | 95:5 |
| 21[f] | **L2** | *t*BuOH/toluene (1:1) | 25 | 87 | 87 | 93:7 |

[a] Determined by $^1$H NMR spectroscopic analysis of the crude mixture. [b] Yield of **3a** isolated by column chromatography on silica gel. [c] Determined by HPLC analysis. [d] Not applicable. [e] Five equivalents of $H_2O$ to **1a** were used. [f] 1.2 equivalents of **2a** were used.

Next, protic solvents were examined despite the expected dissociation of the ligand–substrate hydrogen bonds. Alcoholic solvents, such as EtOH, *i*PrOH, and *t*BuOH, gave much higher conversions and yields, and, interestingly, the enantiocontrol was markedly improved (the *R*/*S* enantiomeric ratio (e.r.) was as high as 83:17 with *i*PrOH; Table 1, entries 7–9). The reaction at 25 °C resulted in even higher enantiocontrol (85:15 e.r.) at the expense of the conversion rate (96 h, 91 % conv.; Table 1, entry 10). Importantly, no reaction occurred with **L1-OMe**, even in the alcoholic solvent (*t*BuOH) (Table 1, entry 11). These results strongly suggest that a directional ligand–substrate hydrogen bond occurs in alcoholic solvents. Furthermore, alcoholic solvent molecules must participate in the enantiocontrol through hydrogen-bonding interactions.

In our effort to optimize the chiral ligand, it appeared that both the reaction rate and enantiocontrol could be improved by introducing sterically demanding hydrocarbon substituents at the α position of the hydroxy group. Consequently, ligand **L2** with a neopentyl group was optimal, thus affording **3a** in 95 % yield of the isolated product with 94:6 e.r. (Table 1, entry 12). The enantioselectivity with **L2** was 95:5 e.r. when the reaction temperature was decreased to 25 °C and was further increased to 96:4 e.r. when *t*BuOH was used as the solvent (Table 1, entries 13 and 14). Interestingly, the addition of a small amount of $H_2O$ (5 equiv to **1a**) increased the enantioselectivity to give (*R*)-**3a** with 94 % *ee* (i.e., 97:3 e.r.; Table 1, entry 15). The role of $H_2O$ is unclear. The amount of alkyne **2a** could be decreased to 1.2 equivalents while leaving the quantitative yield unchanged (Table 1, entry 16). To obtain the *S* isomer of **3a**, the anitipode of **L2** (***ent*-L2**), which was synthesized from a D-proline-based starting material (see the Supporting Information), was successfully applied to this protocol (Table 1, entry 17).

Aprotic solvents, such as toluene and THF, were significantly inferior to the alcoholic solvents for optimizing both the conversion rate and enantiocontrol (Table 1, entries 18 and 19). Mixed solvent systems composed of *t*BuOH and toluene (3:1 or 1:1) gave e.r. values intermediate between those systems with the single components (Table 1, entries 20 and 21).

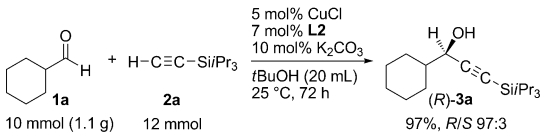


Figure 2. A gram-scale reaction of **1a** and **2a** with a bench-stable catalyst precursor.

Upon scaling up the reaction (i.e., **1a**: 10 mmol, **2a**: 12 mmol) with a lower catalyst loading (Cu: 5 mol %), we confirmed that the air-sensitive copper source CuO*t*Bu could be replaced with a bench-stable $CuCl/K_2CO_3$ system without affecting the yield and enantioselectivity (Figure 2). The addition of $H_2O$ showed no effect under these conditions.

**Substrates**: The range of aldehydes is shown in Table 2 (entries 1–12). The reaction of an aliphatic aldehyde **1b** with a branch at the β position proceeded with high enantioselec-

Table 2. Scope of aldehydes **1** and alkynes **2**.[a]

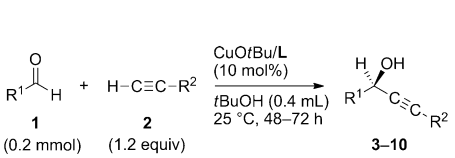


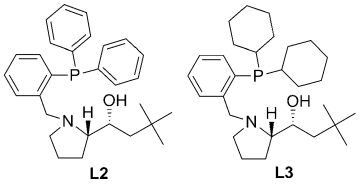


| Entry | $R^1CHO$ **1** | Alkyne **2** | Ligand | Product | Yield [%] | e.r.[b] |
|---|---|---|---|---|---|---|
| 1 | $CyCH_2CHO$ (**1b**) | HC≡CSi*i*Pr$_3$ (**2a**) | **L2** | (*R*)-**3b** | 75 | 95:5 |
| 2 | *i*PrCHO (**1c**) | HC≡CSi*i*Pr$_3$ (**2a**) | **L2** | (*R*)-**3c** | 87 | 93:7 |
| 3 | 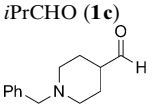 | HC≡CSi*i*Pr$_3$ (**2a**) | **L2** | (*R*)-**3d** | 99 | 97:3 |
| 4 | 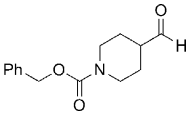 | HC≡CSi*i*Pr$_3$ (**2a**) | **L2** | (*R*)-**3e** | 98 | 97:3 |
| 5 | *t*BuCHO (**1f**) | HC≡CSi*i*Pr$_3$ (**2a**) | **L2** | (*R*)-**3f** | 42 | 86:14 |
| 6 | PhCHO (**1g**) | HC≡CSi*i*Pr$_3$ (**2a**) | **L2** | (*R*)-**3g** | 71 | 89:11 |
| 7 | PhCHO (**1g**) | HC≡CSi*i*Pr$_3$ (**2a**) | **L3** | (*R*)-**3g** | 80 | 95:5 |
| 8 | 3-$MeO_2C$-$C_6H_4CHO$ (**1h**) | HC≡CSi*i*Pr$_3$ (**2a**) | **L3** | (*R*)-**3h** | 93 | 93:7 |
| 9 | 4-F-$C_6H_4CHO$ (**1i**) | HC≡CSi*i*Pr$_3$ (**2a**) | **L3** | (*R*)-**3i** | 91 | 94:6 |
| 10 | 4-Cl-$C_6H_4CHO$ (**1j**) | HC≡CSi*i*Pr$_3$ (**2a**) | **L3** | (*R*)-**3j** | 95 | 95:5 |
| 11 | 3-MeO-$C_6H_4CHO$ (**1k**) | HC≡CSi*i*Pr$_3$ (**2a**) | **L3** | (*R*)-**3k** | 95 | 96:4 |
| 12 | 3-thienyl-CHO (**1l**) | HC≡CSi*i*Pr$_3$ (**2a**) | **L3** | (*S*)-**3l** | 73 | 95:5 |
| 13 | CyCHO (**1a**) | HC≡C*i*Bu (**2b**) | **L2** | (*R*)-**4a** | 92 | 93:7 |
| 14 | CyCHO (**1a**) | HC≡C*t*Bu (**2c**) | **L2** | (*R*)-**5a** | 97 | 93:7 |
| 15 | CyCHO (**1a**) | HC≡$CCH_2N(CH_2Ph)_2$ (**2d**) | **L2** | (*R*)-**6a** | 91 | 92:8 |
| 16 | CyCHO (**1a**) | HC≡$CCMe_2OSiMe_2$*t*Bu (**2e**) | **L2** | (*R*)-**7a** | 96 | 94:6 |
| 17 | CyCHO (**1a**) | HC≡CPh (**2f**) | **L2** | (*R*)-**8a** | 94 | 87:13 |
| 18 | CyCHO (**1a**) | HC≡$CC_6H_4$-4-OMe (**2g**) | **L2** | (*R*)-**9a** | 81 | 91:9 |
| 19 | CyCHO (**1a**) | HC≡$CC_6H_4$-4-$CF_3$ (**2h**) | **L2** | (*R*)-**10a** | 98 | 86:14 |
| 20 | PhCHO (**1g**) | HC≡CPh (**2f**) | **L3** | (*R*)-**8g** | 80 | 94:6 |
| 21 | PhCHO (**1g**) | HC≡$CC_6H_4$-4-OMe (**2g**) | **L3** | (*R*)-**9g** | 84 | 92:8 |
| 22 | PhCHO (**1g**) | HC≡$CC_6H_4$-4-$CF_3$ (**2h**) | **L3** | (*R*)-**10g** | 86 | 91:9 |

[a] Reaction conditions: 48 h (entries 3, 4, 8–11, 13–22), 60 h (entry 12), and 72 h (entries 1, 2, 5–7). $H_2O$ (5 equiv to **1**) was added in entries 1–5. [b] Determined by HPLC analysis.

tivity, but the yield was moderate due to self-condensation of the aldehyde (Table 2, entry 1). On the other hand, α-branched aldehydes (**1c**–**e**) are generally suitable substrates in terms of both yield and enantioselectivity (Table 2, entries 2–4). The tolerance toward N-based functional groups, such as tertiary amino and carbamate groups, is an attractive feature of this protocol. Nevertheless, *t*BuCHO (**1f**) reacted with moderate enantioselectivity (Table 2, entry 5). For the reaction of PhCHO (**1g**), the $Cy_2P$-based ligand **L3** gave higher enantioselectivity (95:5 e.r.) than the $Ph_2P$-based ligand **L2** (Table 2, entries 6 vs. 7). The superiority of **L3** applied over a range of substituted aromatic aldehydes (**1h**–**k**) and a heteroaromatic aldehyde (**1l**) (Table 2, entries 8–12).

Various enantioenriched propargylic alcohols **4a**–**10a** and **8b**–**10b** with different substituents at the alkyne terminus were obtained through copper-catalyzed protocols with **L2** or **L3** (Table 2, entries 13–22). Aliphatic alkynes **2b**–**2e** with different degrees and patterns of branching reacted with **1a** with reasonably high enantioselectivities (Table 2, entries 13–16). Functionalized alkynes such as *N*,*N*-dibenzylpropargylamine (**2d**) and an *O*-protected propargylic alcohol **2e** reacted with high yields and enantioselectivities (**6a**, **7a**; Table 2, entries 15 and 16). Although the aromatic alkynes **2f**–**h** reacted with **1a** in somewhat lower enantioselectivities than the aliphatic alkynes (Table 2, entries 17–19), these alkynes were suitable substrates for the reaction with the aromatic aldehyde **1g** catalyzed by using the Cu/**L3** system (Table 2, entries 20–22).

**Proposed reaction pathway**: A proposed reaction pathway, which accounts for most of the mechanistically important experimental results, is illustrated in Figure 3. This cycle is based on the hydrogen-bond-based, cooperative, six-centered transition-state model shown in Figure 1b. It is to be noted that a nonlinear effect in enantiomeric excess was not observed between **L2** and the product **3a**, thus supporting the monomeric nature of the catalytic species (see Figure S1 in the Supporting Information). Because the reaction was conducted in an alcoholic solvent, participation of an exogenous alcohol molecule through hydrogen bonding was considered throughout the catalytic cycle.

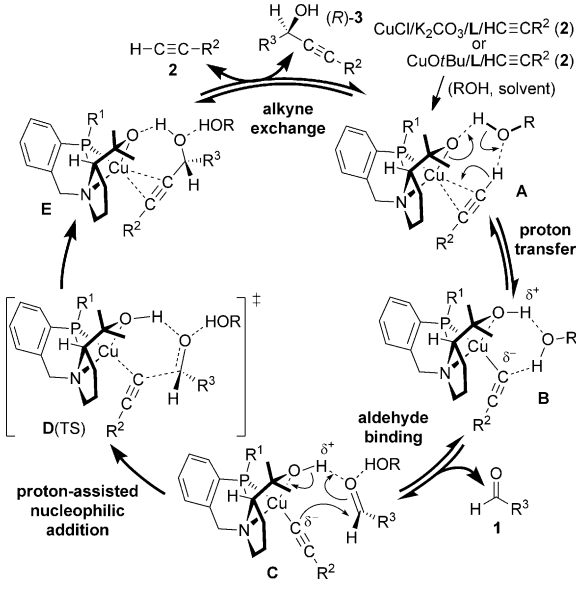


Figure 3. A proposed reaction pathway.

First, a $Cu^I$ alkoxide complex **A** with an $\eta^2$-coordinated alkyne ligand is produced through the reaction between a P,N,OH-ligand **L** and CuO*t*Bu or $CuCl/K_2CO_3$ in the presence of an alkyne (i.e., **2**). The alkoxide oxygen atom and the terminal hydrogen atom of the alkyne likely form a hydrogen-bond bridge with an alcohol molecule, which is either from the alkoxide complex or solvent. The π-complex **A** should be in equilibrium with $\eta^1$-acetylide complex **B** through intramolecular proton transfer. In the acetylide complex **B**, the OH group of **L** stays bound to the Cu atom at the oxygen atom and provides an acidic hydrogen-bond donor site, while the acetylide carbon atom offers a basic (nucleophilic) site. Replacement of the alcohol molecule of **B** with an aldehyde (i.e., **1**) forms a hydrogen-bonded complex **C**, which is a precursor for a nucleophilic addition step. The aldehyde group in **C** should have an interaction with an alcoholic solvent. The proton-assisted, carbon–carbon bond-forming, nucleophilic addition proceeds through a six-centered transition state **D**(TS) to yield the alkoxocopper(I)/propargylic alcohol complex **E**. Finally, the alkyne-exchange equlibrium between **E** and substrate **2** releases the propargylic alcohol **3** to complete the catalytic cycle. The proton-assisted nucleophilic addition should be an enantiodiscriminating step.

**Quantum-mechanical studies**: To understand how the chiral catalysts impart high enantioselectivity, we carried out DFT calculations for the transition states (TSs) of the enantiodiscriminating C–C bond-formation step (cf. **D**(TS) in Figure 3), not only for the modeled reactions between MeCHO and $HC{\equiv}CSiMe_3$ (models 1a and 2a: chiral ligand = **L1** and **L2**, respectively), but also for the reactions between **1a** and $HC{\equiv}CSi\mathit{i}Pr_3$ (**2a**) [model 1b and 2b: ligand = **L1** (Table 1, entry 10) and **L2** (Table 1, entries 14–16 and Figure 2), respectively]. Geometry optimizations were performed at the B3LYP[21,22] level with the TZVP basis set[23] for Cu and with the 6-31G(d) basis set[24] for the other atoms (termed BI basis sets). Single-point energies of the optimized geometries were calculated at the B3LYP-D-(PCM) level[25–27] with the TZVP basis set for the Cu center and with the 6-311+G(d,p) basis set[26] for the other atoms (termed BII basis sets); energy was adjusted to introduce the effects of the solvent polarity of *t*BuOH ($\varepsilon = 12.0$) and empirical dispersion corrections.

First, the TS geometries were optimized for a simplified model (model 1a) with **L1**, MeCHO, and a $C{\equiv}CSiMe_3$ group to investigate the range of conformers (40 for each of the major and minor enantiomers and 80 in total) of the pyrrolidine[28] and P,N-chelate rings with the copper atom at the B3LYP level with a smaller basis set (termed B0 basis sets; see the Supporting Information for details). This process re-

sulted in convergence to eight TS structures for each isomer (see Table S2 in the Supporting Information). The two most meaningful conformers out of the eight were further optimized at the B3LYP level with a larger basis set BI (see Figure S5 in the Supporting Information). Figure 4 shows the most stable structures of TSs that lead to the major (**M**) and

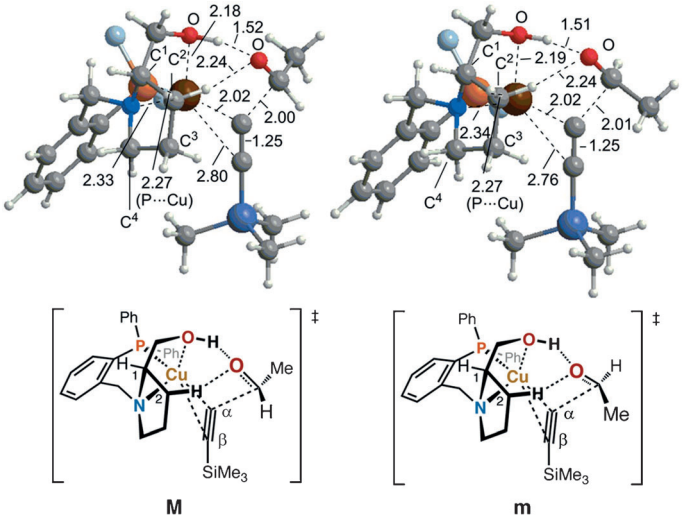


Figure 4. The most stable structures of the major (**M**) and minor (**m**) transition states for model 1a (**L1**, MeCHO, $-C{\equiv}CSiMe_3$). Phenyl groups are shown as light-blue balls for clarity.

minor (**m**) enantiomeric products, in which the pyrrolidine ring adopts an envelope-type conformation with an out-of-plane N atom and an equatorial hydroxymethylene side chain. A reasonable value of 72.9 kJ mol$^{-1}$ was obtained for the Gibbs activation energy of alkynylation through the most stable TS(**M**) (see Figure S7 in the Supporting Information). In contrast, four-centered TSs, in which the carbonyl oxygen atom is directly coordinated to the Cu atom with the OH group of the ligand free from coordination, were greater than 70 kJ mol$^{-1}$ higher in total electronic energy relative to the six-centered TSs (see Table S5 and Figures S8 and S9 in the Supporting Information). Accordingly, for further studies, we decided to consider only six-centered TSs that adopted the pyrrolidine and P,N-chelate-ring conformations as in the most stable TSs of model 1a (Figure 4).

A surprising feature of the TSs of model 1a (Figure 4) is that, in addition to the hydrogen bond between the OH group and aldehyde oxygen atom with H···O atomic distances of 1.52 and 1.51 Å, the pyrrolidine ring has a direct interaction with the carbonyl oxygen atom through a nonclassical $C^2$–H···O hydrogen bond with an H···O atomic distance of 2.24 Å for both TS(**M**) and TS(**m**). Although the C–H bond lengths are normal, the H···O atomic distances are considerably shorter than the sum of van der Waals radii of the H and O atoms (ca. 2.6 Å). Similar $sp^3$-C–H···O interactions are found in organic crystal structures[29] and biomolecules,[30] although they have rarely been referred to in the studies on artificial catalyst systems.[31–37] Other optimized conformers without a $C^2$–H···O hydrogen bond are no less than 16.0 kJ mol$^{-1}$ higher in Gibbs free energy (B3LYP-D-(PCM)/BI//B3LYP/B0; see Table S3 in the Supporting Information). Consequently, the directional two-point hydrogen-bonding orients the carbonyl group. Nevertheless, the **M** and **m** structures are almost equal in stability, and calculations of the Boltzmann distribution at 25 °C from the Gibbs free energies of all the optimized structures for this modeled system give an **M**/**m** abundance ratio (e.r.) as low as 57.4:42.6 (see Table S4 in the Supporting Information).

We then performed calculations for a more advanced model system (model 1b) with **L1**, **1a**, and a $C{\equiv}CSiiPr_3$ group (**2a**-H), which corresponds to the experiment that showed the moderate enantiomeric ratio of 85:15 (Table 1, entry 10). To decrease the cost of the calculations, only a single conformation of the CyCHO molecule and the most stable three conformations of the $SiiPr_3$ moiety were considered; the latter were obtained by conformational analysis of **2a** at the HF/6-31G* level with the Spartan 08 program.[38] The calculations, albeit with considerable ambiguity due to the conformational constraints in the CyCHO molecule, gave a reasonable **M**/**m** abundance ratio of 74.9:25.1 e.r. (see Figure S10 and Table S6 in the Supporting Information).

After preliminary examination of the other simplified model system (model 2a) with the neopentyl-substituted ligand **L2** (see Figure S11 and Table S7 in the Supporting Information), which gave a **M**/**m** ratio of 64.0:36.0 e.r., we performed calculations for a system (i.e., model 2b) with **L2**, **1a**, and a $C{\equiv}CSiiPr_3$ group (**2a**-H). These conditions correspond to the optimal reaction conditions in the experiments (Table 1, entries 13–15, and Figure 2). Geometry optimizations were conducted for 27 conformers for each of TS(**M**) and TS(**m**), with different conformations of the neopentyl group (×3), the CyCHO molecule (×3), and the $SiiPr_3$ group (×3; see Table S8 and Figure S12 in the Supporting Information). The most stable structures of **M** and **m** are shown in Figure 5a. The **M**/**m** abundance ratio based on the Boltzmann distribution at 25 °C from the Gibbs free energies of all the optimized structures was 96.9:3.1 e.r. (see Table S8 in the Supporting Information) in accord with the efficient enantiocontrol (up to 97:3 e.r. in *t*BuOH at 25 °C) with the Cu/**L2** system in the experiments.

The neopentyl group of **L2** is relatively distant from both the alkyne and aldehyde substrates, thus overhanging the Cu-bound hydroxy group with its *t*Bu hammerhead: the hydrogen atom on the carbon atom at the α position to the OH group and the OH oxygen atom have van der Waals contacts with the nearest *t*Bu hydrogen atoms (Figure 5a). The *P*-phenyl groups (omitted in Figure 5a) are also located in regions where no direct interaction with the substrates occurs. Despite a lack of chiral ligand–substrate steric interactions (which is unusual in enantioselective catalysis), the directional two-point hydrogen bond arranges the aldehyde carbonyl group asymmetrically in a well-defined manner. As a result, the difference in the steric environment around the aldehyde between TS(**M**) and TS(**m**) is evident, as shown in the views from the plane of the aldehyde along the develop-

  

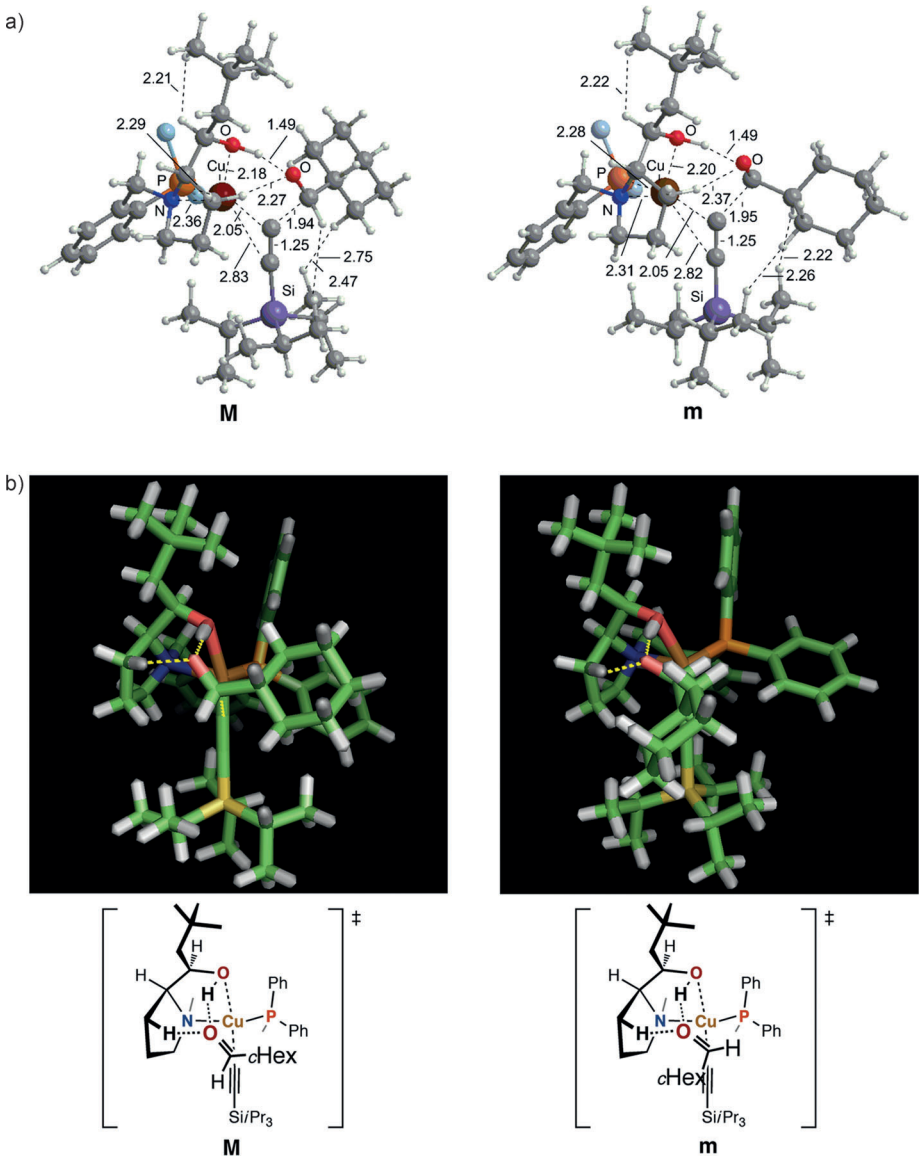


Figure 5. The most stable structures of the **M** and **m** transition states for model 2b (**L2**, **1a**, and **2a**-H). a) Side views (the phenyl groups are shown as light-blue balls for clarity). b) Views (from the front) from the plane of the aldehyde along the developing C–C bond.

ing C–C bond (Figure 5b). The Cy substituent in TS(**M**) is arranged perpendicularly to the axis of the acetylide, whereas that it is eclipsed in the TS(**m**). Consequently, TS(**m**) encounters larger steric repulsion between the Cy substituent of the aldehyde and Si*i*Pr$_3$ substituent of the alkyne. The neopentyl group in **L2**, which is distal to the substrates, might play the role of an anchor to enhance the directionality of the hydrogen bonds, thus producing a well-defined chiral reaction environment.

To confirm that the sp$^3$-C–H···O hydrogen bond exists even in an alcoholic solvent, we attached a single MeOH molecule to the aldehyde C=O oxygen atom of the most-stable conformer of TS(**M**) of model 2b through a hydrogen bond (cf. **D**(TS) in Figure 3). This step caused only a small structural change in the TS except for the elongation of the C$^2$–H···O and O–H···O hydrogen-bonding distances by approximately 5% (see Figure S13 in the Supporting Information). Although the possibility of a certain degree of overestimation of the sp$^3$-C–H···O hydrogen bond is not ruled out, it is difficult to explain the efficient enantiocontrol without considering this secondary interaction (see Figure S4 in the Supporting Information for various higher energy conformers without a C-H···O hydrogen bond in model 1a).

## Conclusion

A copper-catalyzed enantioselective alkynylation of aldehydes with terminal alkynes with prolinol-based hydroxy amino phosphane chiral ligands has been developed. This reaction presents a case in which ligand–substrate hydrogen-bonding interactions cooperate with a metal center in protic solvents. Quantum-mechanical calculations show the occurrence of a nonclassical sp$^3$-C–H···O hydrogen bond as a secondary interaction between the ligand and the carbonyl substrate, which results in highly directional catalyst–substrate two-point hydrogen bonding. The enantioselective catalysis is applicable for both aliphatic and aromatic aldehydes in combination with various alkynes with different terminal substituents, thus providing a useful method to prepare enantioenriched propargylic alcohols, thus eliminating the problems of existing systems, such as a limited substrate range or the use of precious metals and organic bases in large quantities.[12–16] Catalyst–substrate hydrogen-bonding interactions in protic solvents and sp$^3$-C–H···O hydrogen bonds would be useful new concepts to understand the mechanisms of cooperative asymmetric catalysis and for future catalyst design. On the other hand, the question of why aliphatic aldehydes and aromatic aldehydes favor different P substituents ($PPh_2$ vs. $PCy_2$) and of how the alcoholic solvents participate in the catalysis remain to be elucidated.

## Experimental Section

**Procedure for a gram-scale reaction of 1a and 2a with a bench-stable catalyst precursor (Figure 2)**: CuCl (49.5 mg, 0.5 mmol), $K_2CO_3$ (138 mg, 1.0 mmol), and **L2** (312 mg, 0.7 mmol) were placed in a two-necked round-bottom flask containing a magnetic stirring bar. The flask was sealed with a rubber septum, evacuated, and filled with argon. *t*BuOH (20 mL) was added to the flask, and the mixture was stirred at 25 °C for 5 min. Alkyne **2a** (2.7 mL, 12 mmol) and aldehyde **1a** (1.2 mL, 10 mmol) were added to the flask. After stirring for 72 h at 25 °C, the reaction mixture was concentrated, and the residue was subjected to silica gel chromatography (hexane/EtOAc 95:5) to give **3a** (2.86 g, 9.7 mmol) in 97% yield.

## Acknowledgements

This work was supported by CREST (JST) to M.S and by ACT-C (JST) to M.S. and S.M. We thank MEXT for the financial support through the Global COE grant (Project No. B01: Catalysis as the Basis for Innovation in Materials Science) to M.S. and the Grant-in-Aid for Scientific Research on Innovative Areas "Molecular Activation Directed toward Straightforward Synthesis" to S.M. The generous allotment of computation time from the Research Center for Computational Science (RCCS; National Institutes of Natural Sciences, Japan) is also gratefully acknowledged.

[1] G. A. Jeffrey, *An Introduction to Hydrogen Bonding*, Oxford University Press, Oxford, **1997**.
[2] M. Sawamura, Y. Ito, *Chem. Rev.* **1992**, *92*, 857–871.
[3] T. Ikariya, K. Murata, R. Noyori, *Org. Biomol. Chem.* **2006**, *4*, 393–406.
[4] A. G. Doyle, E. N. Jacobsen, *Chem. Rev.* **2007**, *107*, 5713–5743.
[5] T. Akiyama, *Chem. Rev.* **2007**, *107*, 5744–5758.
[6] T. Hayashi, K. Kanehira, T. Hagihara, M. Kumada, *J. Org. Chem.* **1988**, *53*, 113–120.
[7] Y. Ito, M. Sawamura, T. Hayashi, *J. Am. Chem. Soc.* **1986**, *108*, 6405–6406.
[8] S. Morikawa, K. Michigami, H. Amii, *Org. Lett.* **2010**, *12*, 2520–2523.
[9] A. P. Brogan, T. J. Dickerson, K. D. Janda, *Angew. Chem.* **2006**, *118*, 8278–8280; *Angew. Chem. Int. Ed.* **2006**, *45*, 8100–8102.
[10] Y. Hayashi, *Angew. Chem.* **2006**, *118*, 8281–8282; *Angew. Chem. Int. Ed.* **2006**, *45*, 8103–8104.
[11] The Noyori–Ikariya asymmetric transfer hydrogenation of ketones catalyzed by transition-metal amides and related catalysis are important exceptions; see ref. [3] and C. Wang, X. Wu, J. Xiao, *Chem. Asian J.* **2008**, *3*, 1750–1770.
[12] A review on the enantioselective alkynylation of carbonyl compounds and imines: B. M. Trost, A. H. Weiss, *Adv. Synth. Catal.* **2009**, *351*, 963–983.
[13] N. K. Anand, E. M. Carreira, *J. Am. Chem. Soc.* **2001**, *123*, 9687–9688.
[14] R. Takita, K. Yakura, T. Ohshima, M. Shibasaki, *J. Am. Chem. Soc.* **2005**, *127*, 13760–13761.
[15] a) Y. Asano, K. Hara, H. Ito, M. Sawamura, *Org. Lett.* **2007**, *9*, 3901–3904; b) Y. Asano, H. Ito, K. Hara, M. Sawamura, *Organometallics* **2008**, *27*, 5984–5996.
[16] J. Ito, R. Asai, H. Nishiyama, *Org. Lett.* **2010**, *12*, 3860–3862.
[17] J. W. Bode, E. M. Carreira, *J. Am. Chem. Soc.* **2001**, *123*, 3611–3612.
[18] J. A. Marshall, M. P. Bourbeau, *Org. Lett.* **2003**, *5*, 3197–3199.
[19] For a review on the enantioselective direct alkynylation of imines with terminal alkynes, see: P. de Armas, D. Tejedor, F. García-Tellado, *Angew. Chem.* **2010**, *122*, 1029–1032; *Angew. Chem. Int. Ed.* **2010**, *49*, 1013–1016.
[20] "TRAP" is an abbreviation for "Trans-chelating chiral phosphane". See: a) M. Sawamura, H. Hamashima, Y. Ito, *Tetrahedron: Asymmetry* **1991**, *2*, 593–596; b) M. Sawamura, H. Hamashima, M. Sugawara, R. Kuwano, Y. Ito, *Organometallics* **1995**, *14*, 4549–4558.
[21] A. D. Becke, *J. Chem. Phys.* **1993**, *98*, 5648–5652.
[22] C. Lee, W. Yang, R. G. Parr, *Phys. Rev. B* **1988**, *37*, 785–789.
[23] A. Schäfer, C. Huber, R. Ahlrichs, *J. Chem. Phys.* **1994**, *100*, 5829–5835.
[24] W. J. Hehre, L. Radom, P. v. R. Schleyer, J. A. Pople, *Ab Initio Molecular Orbital Theory*, Wiley, New York, **1986**.
[25] S. Grimme, *J. Comput. Chem.* **2006**, *27*, 1787–1799.
[26] S. Miertuš, E. Scrocco, J. Tomasi, *Chem. Phys.* **1981**, *55*, 117–129.
[27] J. Tomasi, B. Mennucci, R. Cammi, *Chem. Rev.* **2005**, *105*, 2999–3093.
[28] L. Carballeira, I. Pérez-Juste, C. VanAlsenoy, *J. Phys. Chem. A* **2002**, *106*, 3873–3884.
[29] G. R. Desiraju, *Acc. Chem. Res.* **1996**, *29*, 441–449.
[30] P. Chakrabarti, S. Chakrabarti, *J. Mol. Biol.* **1998**, *284*, 867–873.
[31] For formyl C–H···O hydrogen bonds in enantioselective Lewis acid-catalyzed reactions of aldehydes, see: E. J. Corey, T. W. Lee, *Chem. Commun.* **2001**, 1321–1329.
[32] TS models involving hydrogen bonds between an N-adjacent $sp^3$ C–H bond of *N*-acylimidazolinium salts and a carboxylate oxygen atom have been proposed for the enantioselective acyl transfer catalysis; see: I. Shiina, K. Nakata, K. Ono, Y. Onoda, M. Itagaki, *J. Am. Chem. Soc.* **2010**, *132*, 11629–11641.
[33] Hydrogen-bonding interactions between an N-adjacent $sp^2$-C–H bond and a carboxylate oxygen atom have been proposed for acyl transfer catalysis with 4-(*N*,*N*-dimethylamino)pyridine (DMAP); see: S. Xu, I. Held, B. Kempf, H. Mayr, W. Steglich, H. Zipse, *Chem. Eur. J.* **2005**, *11*, 4751–4757.
[34] C–H···O interactions in *cinchona* alkaloid-catalyzed enantioselective methanolysis of *meso*-cyclic anhydrides: H. Yang, M. W. Wong, *J. Am. Chem. Soc.* **2013**, *135*, 5808—5818.
[35] For $sp^2$-C–H···O interactions in enantioselective thiourea organocatalysis, see: K. M. Lippert, K. Hof, D. Gerbig, D. Ley, H. Hausmann, S. Guenther, P. R. Schreiner, *Eur. J. Org. Chem.* **2012**, 5919—5927.
[36] List proposed the occurrence of $sp^3$-C–H···O=P interactions in the transition state of the Brønsted acid-catalyzed enantioselective $S_N2$-type *O*-alkylation reactions; the C–H bond is located at the pentagonal carbon center with a partial positive charge; see: I. Čorić, J. H. Kim, T. Vlaar, M. Patil, W. Thiel, B. List, *Angew. Chem.* **2013**, *125*, 3574–3577; *Angew. Chem. Int. Ed.* **2013**, *52*, 3490–3493.
[37] For X-ray crystal structures involving (2-pyridyl)$_3$C–H···$Cl^-$ interactions in $Pd^{IV}$ complexes coordinated with a tridentate pyridine ligand, see: A. Maleckis, J. W. Kampf, M. S. Sanford, *J. Am. Chem. Soc.* **2013**, *135*, 6618–6625.
[38] Spartan 08, Wavefunction, Inc., Irvine, CA, **2008**.

Received: April 5, 2013
Revised: June 27, 2013
Published online: ■■ ■■, 0000

  

Asymmetric Synthesis

*T. Ishii, R. Watanabe, T. Moriya, H. Ohmiya, S. Mori,* M. Sawamura** ..... ▮▮▮▮–▮▮▮▮

**Cooperative Catalysis of Metal and O−H···O/sp$^3$-C−H···O Two-Point Hydrogen Bonds in Alcoholic Solvents: Cu-Catalyzed Enantioselective Direct Alkynylation of Aldehydes with Terminal Alkynes**

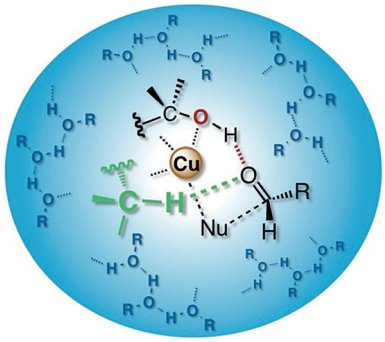


**Efficient enantioselective** direct carbonyl addition of terminal alkynes is achieved through ligand–substrate two-point hydrogen bonds consisting of O−H···O and sp$^3$-C−H···O interactions that cooperate with copper in alcoholic solvents (see picture).